Stoichiometrically Sensitized Decarboxylation Occurring in the Two-Component Molecular Crystals of Aza Aromatic Compounds and Aralkyl Carboxylic Acids

Hideko Koshima,*,† Kuiling Ding,† Yosuke Chisaka,† Teruo Matsuura,† Ikuko Miyahara,‡ and Ken Hirotsu‡

Contribution from the Department of Materials Chemistry, Faculty of Science and Technology, Ryukoku University, Seta, Otsu 520-21, Japan, and Department of Chemistry, Faculty of Science, Osaka City University, Sugimoto, Sumiyoshi, Osaka 558, Japan

Received April 11, 1997[⊗]

Abstract: Highly selective photodecarboxylation could be achieved by utilizing a series of two-component molecular crystals of aralkyl carboxylic acids such as 3-indolepropionic acid (**a**) and 1-naphthylacetic acid (**b**) combined with acridine (**1**) or phenanthridine (**2**) as an electron acceptor. The 1:1 hydrogen bonded crystals were prepared by recrystallization from the solutions. Irradiation of the crystals at −70 °C caused highly selective decarboxylation to give corresponding decarboxylated compounds alone in nearly quantitative yields, due to a smaller thermal motion of the radical species in the crystal lattice. Upon irradiating a crystal, a carboxylate radical and hydroacridine or hydrophenanthridine radical are produced via electron transfer from the acid to **1** or **2** and subsequent proton transfer followed by decarboxylation. Next hydrogen abstraction by an active aralkyl radical occurs in highest priority over the shortest distance of 3.2−3.5 Å resulting in the formation of a corresponding decarboxylated product and the regeneration of **1** or **2**. Occurrence of radical coupling is low due to the longer coupling distance of 4.5−6.5 Å estimated from the crystallographic data of the starting two-component molecular crystals. The hydrogen abstraction path in the crystal lattice could be confirmed by the reaction of a deuterated crystal **1·bD** in which the CO_2H group was replaced by CO_2D, giving a deuterated 1-methyl(CH_2D)naphthalene as a product. Regeneration of **1** or **2** means that the acceptor plays the role of a stoichiometrical sensitizer, which can act in only one cycle, retaining the initial crystal structure. Such a stoichiometrical sensitization is a novel photochemical process, which occurs specifically in the solid state.

Introduction

One of the features of solid state photoreactions is the higher product selectivity due to the restricted motion of molecules in the crystal lattice than in solution photoreactions. Since the rigorous analysis of topochemical [2 + 2] photocycloadditions in the solid state by Cohen and Schmidt,[1] a large number of highly selective photoreactions of one-component molecular crystals have been reported. However, the reaction types documented most frequently are generally limited to [2 + 2] cycloaddition and intramolecular reactions.[2,3] In the field of solution photochemistry, a large number of photoinduced electron transfer (PET) reactions are already known.[4] Recently we have shown that various types of solid state bimolecular reactions via PET also can be caused by irradiating two-component molecular crystals of which electron donor and acceptor species are combined.[5]

The photodecarboxylation of organic carboxylic acids in solution is known to occur via PET mechanisms,[6] using various acceptors such as aza aromatic compounds,[7−9] polycyanoaromatics,[10,11] or dye sensitizers.[8] However, the product selectivities are not necessarily high due to the co-occurrence of subsequent radical coupling in solutions. We have reported in a preliminary communication that a highly selective and efficient photodecarboxylation occurs in a two-component molecular crystal of phenanthridine and 3-indoleacetic acid at low temperature.[12] Furthermore, photoirradiation of two-component molecular crystals of an aralkyl carboxylic acid combined with an electron acceptor caused decarboxylative condensation between the two components with remarkable selectivities in comparison to those observed in solution.[12−16] Thus, chirality of *S*-(+)-2-(6-methoxy-2-naphthyl)propanoic acid in a CT

† Ryukoku University.

‡ Osaka City University.

[⊗] Abstract published in *Advance ACS Abstracts,* October 1, 1997.

(1) (a) Cohen, M. D.; Schmidt, G. M. *J. Chem. Soc.* **1964**, 1996−2000. (b) Schmidt, G. M. *J. Pure Appl. Chem.* **1971**, *27*, 647−678.

(2) Desiraju, G. R., Ed. *Organic Solid State Chemistry*; Elsevier: Amsterdam, 1987.

(3) Ohashi, Y., Ed. *Reactivity in Molecular Crystals*; VCH: Weinheim, 1993.

(4) Fox, M. A., Chanon, M., Eds. *Photoinduced Electron Transfer*; Elsevier: Amsterdam, 1988; Part C.

(5) (a) Koshima, H.; Matsuura, T. *Kokagaku* **1995**, *19*, 10−20. (b) Koshima, H.; Matsuura, T. *J. Photochem. Photobiol. A: Chem.* **1996**, *100*, 85−91. (c) Koshima, H.; Wang, Y.; Matsuura, T.; Miyahara, I.; Mizutani, H.; Hirotsu, K.; Asahi, T.; Masuhara, H. *J. Chem. Soc., Perkin Trans. 2* **1997**, 2033−2037.

(6) Budac, C.; Wan, P. *J. Photochem. Photobiol. A: Chem.* **1994**, *67*, 135−166.

(7) Noyori, R.; Kato, M.; Kawanishi, M.; Nozaki, H. *Tetrahedron* **1969**, *25*, 1125−1136.

(8) Brimage, D. R. G.; Davidson, R. S.; Steiner, P. R. *J. Chem. Soc., Perkin Trans. 1* **1973**, 526−529.

(9) (a) Okada, K.; Okubo, K.; Oda, M. *Tetrahedron Lett.* **1989**, *30*, 6733−6736. (b) Okada, K.; Okubo, K.; Oda, M. *J. Photochem. Photobiol. A: Chem.* **1991**, *57*, 265−277.

(10) Tsujimoto, K.; Nakao, N.; Ohashi, M. *J. Chem. Soc., Chem. Commun.* **1992**, 366−367.

(11) Libman, J. *J. Am. Chem. Soc.* **1975**, *97*, 4139−4141.

(12) Koshima, H.; Ding, K.; Matsuura, T. *J. Chem. Soc., Chem. Commun.* **1994**, 2053−2054.

(13) Koshima, H.; Ding, K.; Chisaka, Y.; Matsuura, T. *Tetrahedron: Asymmetry* **1995**, *6*, 101−104.

(14) Koshima, H.; Ding, K.; Chisaka, Y.; Matsuura, T. *J. Am. Chem. Soc.* **1996**, *118*, 12059−12065.

S0002-7863(97)01156-6 CCC: $14.00

Chart 1

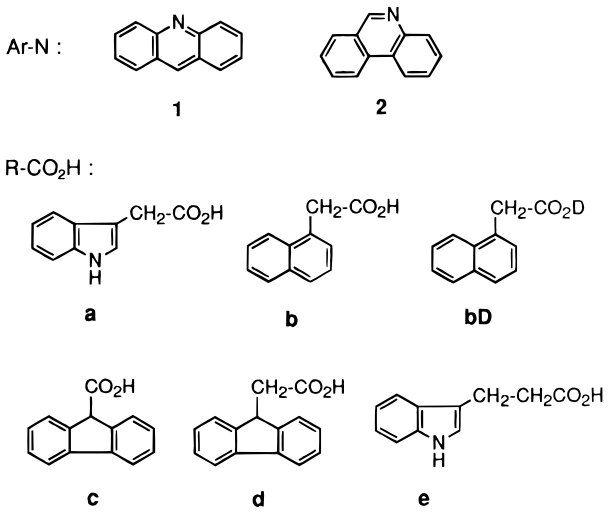

Two-component molecular crystals :

1·a	**1·b**	**1·bD**	**1·c**	**1·d**	
2·a	**2·b**		**2·c**		**2·e**

crystal with 1,2,4,5-tetracyanobenzene was retained in the decarboxylative condensation product,[13] and an absolute asymmetric synthesis using a chiral two-component molecular crystal formed from achiral diphenylacetic acid and acridine was achieved by the enantioselective decarboxylative condensation.[14]

We describe here how the highly selective photodecarboxylation can be extended to a series of two-component molecular crystals of aralkyl carboxylic acids combined with aza aromatic compounds. On the basis of the correlation between crystal structure and selectivity, we have established the new concept[12] of stoichiometric sensitization.

Results and Discussion

Two-Component Molecular Crystals. Acridine (**1**) and phenanthridine (**2**) were chosen as aza aromatic compounds and 3-indoleacetic acid, (**a**) 1-naphthylacetic acid (**b**), 9-fluoreneacarboxylic acid (**c**), 9-fluoreneacetic acid (**d**), and 3-indolepropionic acid (**e**) as aralkyl carboxylic acids (Chart 1). Deuterated 1-naphthylacetic acid (**bD**), of which the CO_2H carboxylic acid group was exchanged to CO_2D, was also used. Nine two-component molecular crystals were prepared by recrystallization from the equimolar solutions of both components. The solvents, melting points, and elemental analyses of the two-component-molecular crystals are summarized in Table 1. The molar ratio of all the crystals is 1:1. The melting points of **1·a**, **1·c**, **2·c**, and **2·e** are between those of the component crystals, while the others are lower than those of the two components. The melting point of deuterated **1·bD** (74−76 °C) is slightly lower than that of **1·b** (77−79 °C).

Eight two-component molecular crystals were submitted to X-ray crystallographic analysis (Table 2). A high-quality single crystal of **2·b** for X-ray analysis could not be obtained. Seven crystals belong to achiral space groups, except **2·e** which crystallized in a chiral space group ($P2_1$). In the crystal lattice, two-component molecules are connected through the O−H···N hydrogen bonding between the hydroxyl group of **a**−**e** and the N atom of **1** or **2**. In the case of the crystals containing **a** or **e**, additional N−H···O═C hydrogen bonding is formed between the N−H group of the indole ring and the carbonyl group of the adjacent molecule of **a** or **e**. Table 3 summarizes the length, angle, and dihedral angle data of hydrogen bonding pairs and their head-to-tail or head-to-head stacking manner in the crystal lattice.

Figure 1 shows the representative molecular packing diagrams. In the case of **1·b**, hydrogen bonding pairs of **1** and **b** are stacked head-to-tail and four pairs are packed in a unit cell. Surprisingly, the crystal **1·bD** of which CO_2H was replaced by CO_2D resulted in a change of crystal system from monoclinic (**1·b**) to triclinic (**1·bD**) (Figure 1 and Table 2). The H···N length of hydrogen bonding in **1·bD** (1.77 Å) is slightly longer than that in **1·bD** (1.42 Å) due to the weaker hydrogen bonding ability of deuterium than hydrogen. The conformations of hydrogen bonding pairs between **1·b** and **1·bD** are different; the dihedral angles of the carboxyl plane and the acridine plane are considerably different (Table 3). However, the molecular packing arrangements in head-to-tail pairs seem to be rather similar.

In the crystal lattice of **2·a** (Figure 1), a linear chain structure is formed through the N−H···O═C hydrogen bondings among the molecules of **a**, which is also connected with the molecules of **2** by another O−H···N hydrogen bonding. Further, the molecules of **2** are stacked head-to-tail and parallel, with a centrosymmetry in the crystal lattice. In the **2·c** case, the hydrogen bonding pairs arrange head-to-head to form a column structure in the crystal lattice.

Solution and Solid State Photoreaction. Irradiation of solutions of aza aromatic compounds and carboxylic acids in acetonitrile or benzene caused decarboxylation followed by radical coupling to give typically four products. The results are shown in Scheme 1 and Table 4. They are decarboxylated product **3**, condensation product **4**, the dimer of **3** (**7**), and the dimer of **1** (**8**) or **2** (**9**). In some cases, dehydrogenated condensation product **5** or **6** was obtained. Namely, all the possible radical coupling products formed in low selectivities due to the high mobility of intermediate radical species in the solution.

Solid state irradiation of the two-component molecular crystals caused selective decarboxylation except for **2·e** to give the corresponding decarboxylated product **3** in high yields as the main product (Scheme 1). Table 5 summarizes the results at various irradiation temperatures in the range −70 to 15 °C. The condensation product **4** and dehydrogenated condensation products **5** or **6** were obtained as the minor products. The dimers **7**, **8**, and **9** were not produced at all. The high product selectivities are due to the restricted motion of radical species in the crystal lattice, very different from those in solution (Table 4). Lowering the irradiation temperature led to an increase in the selectivities due to a smaller thermal motion of the radical species. In particular, irradiation at −70 °C of **1·c**, **1·d**, **2·a**, and **2·c** caused completely selective decarboxylation to give the corresponding decarboxylated product alone, not being accompanied by any consumption of **1** and **2**.

However, the crystal **2·e** had no photoreactivity to result in complete recovery of the starting materials. The reason is probably due to the very fast back electron transfer of the indolepropionic acid radical cation.

Solid State Reaction Mechanism. How does the photoreaction occur with high product selectivities in the crystal lattice?

(15) Koshima, H.; Ding, K.; Chisaka, Y.; Matsuura, T.; Ohashi, Y.; Mukasa, M. *J. Org. Chem.* **1996**, *61*, 2352−2357.
(16) Koshima, H.; Ding, K.; Miura, T.; Matsuura, T. *J. Photochem. Photobiol. A: Chem.* **1997**, *104*, 105−112.
(17) Koshima, H.; Hayashi, E.; Matsuura, T.; Tanaka, K.; Toda, F.; Kato, M.; Kiguchi, M. *Tetrahedron Lett.* **1997**, *38*, 5009−5017.

Table 1. Characterization of the Two-Component Molecular Crystals of Aza Aromatic Compounds and Aralkyl Carboxylic Acids

				elemental anal					
				calcd (%)			found (%)		
crystal (color)	solvent	melting point (°C)	formula (molar ratio)	C	H	N	C	H	N
1·a (yellow)	MeCN	127−129	$C_{23}H_{18}N_2O_2$ (1:1)	77.95	5.12	7.90	77.80	5.38	7.89
1·b (yellow)	benzene−cyclohexane (1:1)	77−79	$C_{25}H_{19}NO_2$ (1:1)	82.17	5.24	3.83	82.09	5.41	3.79
1·bD (yellow)	benzene−cyclohexane (1:1)	74−76	$C_{25}H_{18}DNO_2$ (1:1)	81.94	4.96	3.82	82.11	5.25	3.71
1·c (yellow)	MeOH	135−138	$C_{27}H_{19}NO_2$ (1:1)	83.27	4.92	3.60	83.40	5.10	3.60
1·d (yellow)	MeCN	100−102	$C_{28}H_{21}NO_2$ (1:1)	85.35	5.25	3.47	83.40	5.40	3.39
2·a (colorless)	EtOAc	96−98	$C_{23}H_{18}N_2O_2$ (1:1)	77.95	5.12	7.90	78.06	5.27	7.92
2·b (colorless)	MeOH	83−85	$C_{25}H_{19}NO_2$ (1:1)	82.17	5.24	3.83	82.42	5.44	3.72
2·c (colorless)	EtOAc	128−130	$C_{27}H_{19}NO_2$ (1:1)	83.27	4.92	3.60	83.48	5.11	3.48
2·e (yellow)	MeCN	112−114	$C_{24}H_{20}N_2O_2$ (1:1)	78.23	5.47	7.61	78.06	5.58	7.63

Table 2. X-ray Crystallographic Data for the Two-Component Molecular Crystals and the Products

	1·a	**1·b**	**1·bD**	**1·c**	**1·d**	**2·a**[a]	**2·c**	**2·e**[b]	**4c-2**	**5a·C_6H_{12}**
formula	$C_{23}H_{18}N_2O_2$	$C_{25}H_{19}NO_2$	$C_{25}H_{18}DNO_2$	$C_{27}H_{19}NO_2$	$C_{28}H_{21}NO_2$	$C_{23}H_{18}N_2O_2$	$C_{27}H_{19}NO_2$	$C_{24}H_{20}N_2O_2$	$C_{26}H_{16}N$	$C_{28}H_{28}N_2$
fw	353.41	365.45	366.43	389.45	403.48	354.41	389.45	368.43	342.42	392.54
space group	P_{bca}	$P2_1/c$	$P\bar{1}$	$P2_1/n$	$P2_1/c$	$P\bar{1}$	$P2_1/n$	$P2_1$	$P2_1/n$	P_{nma}
a (Å)	19.496(4)	10.001(1)	9.354(1)	24.22(1)	12.165(7)	8.5082(5)	4.71(3)	13.251(1)	12.760(1)	17.014(3)
b (Å)	24.864(5)	23.584(6)	13.333(2)	14.883(9)	8.945(6)	13.407(1)	16.85(1)	5.327(1)	14.789(1)	14.239(8)
c (Å)	7.560(3)	8.115(2)	8.244(1)	4.936(3)	19.244(7)	8.4683(9)	25.111(7)	13.6091(7)	19.2786(8)	9.537(3)
α (deg)	90.0	90.0	106.85(1)	90.0	90.0	103.018(7)	90.0	90.0	90.0	90.0
β (deg)	90.0	101.654	104.44(1)	106.01	91.33	106.269(6)	91.9(1)	104.779(7)	92.642(5)	90.0
γ (deg)	90.0	90.0	81.86(1)	90.0	90.0	81.260(6)	90.0	90.0	90.0	90.0
V (Å^3)	3644(1)	1874.7	950.2(3)	1940(2)	2093(1)	899.4(1)	1990(11)	928.9(2)	3634.2(3)	2310(2)
Z	8	4	2	4	4	2	4	2	8	4
ρ_{calcd} (g cm^{-3})	1.281	1.295	1.277	1.33	1.280	1.309	1.299	1.317	1.252	1.128
radiation	Mo Kα	Mo Kα	Mo Kα	Mo Kα	Mo Kα	Mo Kα	Mo Kα	Cu Kα	Cu Kα	Mo Kα
absorp coeff (cm^{-1})	0.83	0.82	0.81	0.98	0.80	0.84	0.82	6.74	5.55	0.65
$2\theta_{max}$ (deg)	50.0	50.0	50.0	50.0	50.0	55.0	50.0	120.0	120.1	50.2
no. of reflns measd	3680	3749	3418	3425	4141	4403	4118	3244	5938	2404
no. of observations	2298	1567	2371	1999	2429	3023	1954	2708	4512	1461
no. of variables	317	330	257	348	281	251	348	334	602	140
R	0.041	0.050	0.046	0.054	0.052	0.051	0.040	0.033	0.046	0.099
R_w	0.028	0.062	0.073	0.079	0.048	0.081	0.031	0.052	0.075	0.108

[a] Reference 12. [b] Reference 17.

Table 3. Detail Data of Hydrogen Bonding Pairs

	1·a	**1·b**	**1·bD**	**1·c**	**1·d**	**2·a**	**2·c**	**2·e**
H-bonding (O−H···N)								
H···N (Å)	1.53	1.42	1.77[a]	1.69	1.64	1.68	1.50	1.51
O···N (Å)	2.60	2.64	2.69	2.72	2.67	2.64	2.65	2.64
O−H···N (deg)	179	175	154[a]	167	168	168	169	171
H-bonding (N−H···O═C)								
H···O (Å)	2.11					2.01		2.09
N···O (Å)	2.92					2.91		2.93
N−H···O (deg)	151					154		161
dihedral angle of H-bonding pair (deg)								
R/COO	64.0	68.6	78.9	64.5	152.2	89.9	59.6	77.1
NAr/COO	93.1	65.2	15.5	33.5	51.3	30.0	25.7	2.2
NAr/R	102.7	89.8	85.1	83.7	113.2	84.7	65.1	78.3
stacking manner of H-bonding pairs[b]	h-t	h-t	h-t	h-h	h-t	h-t	h-h	h-h

[a] H is exchanged to D. [b] The terms h-t and h-h mean head-to-tail and head-to-head stacking, respectively, where the nitrogen atom side of each heteroaromatic refers to head and the other side to tail.

Scheme 2 shows the possible reaction mechanism. Irradiation of a crystal excites **1** or **2** followed by electron transfer from the acid to **1** or **2** to afford an anion radical (**10**) and a cation radical (**11**). Then proton transfer can give a carboxylate radical (**12**) and a hydroacridine radical (**13**) or hydrophenanthridine radical (**14**), which are shown by the most favorable canonical forms. Next, decarboxylation of **12** produces a ·CH_2− aralkyl radical (**15**). Finally, hydrogen abstraction can occur from the N−H of **13** or **14** by the active radical **15** to result in the formation of a decarboxylated product **3** and the regeneration of **1** or **2**, while radical coupling between **15** and **13** or **14** gives a condensation product **4**.

Although these processes inevitably lead to the alteration of the crystal lattice, the radical species can move a little in their lifetimes to lead to hydrogen abstraction and radical coupling. The reaction paths can be discussed on the basis of crystallographic data of two-component molecular crystals such as the estimated distances in Table 6. The occurrence of hydrogen abstraction in higher priority than radical coupling can be explained from the shorter distances for hydrogen abstraction (3.2−3.5 Å) than those for radical coupling (4.5−6.5 Å). Furthermore, the hydrogen atom is very small in contrast to the large size of **13** or **14**, implying its higher mobility in the solid state. Figure 2 illustrates the reaction paths occurring in the crystal lattice. In all the crystals except unreactive **2·e**, hydrogen abstraction occurs between radical species **13** or **14** (H1) and **15** (C1), which are derived from a pair of hydrogen bonds since the C1- - -H1 distance (3.2−3.5 Å) is shortest in

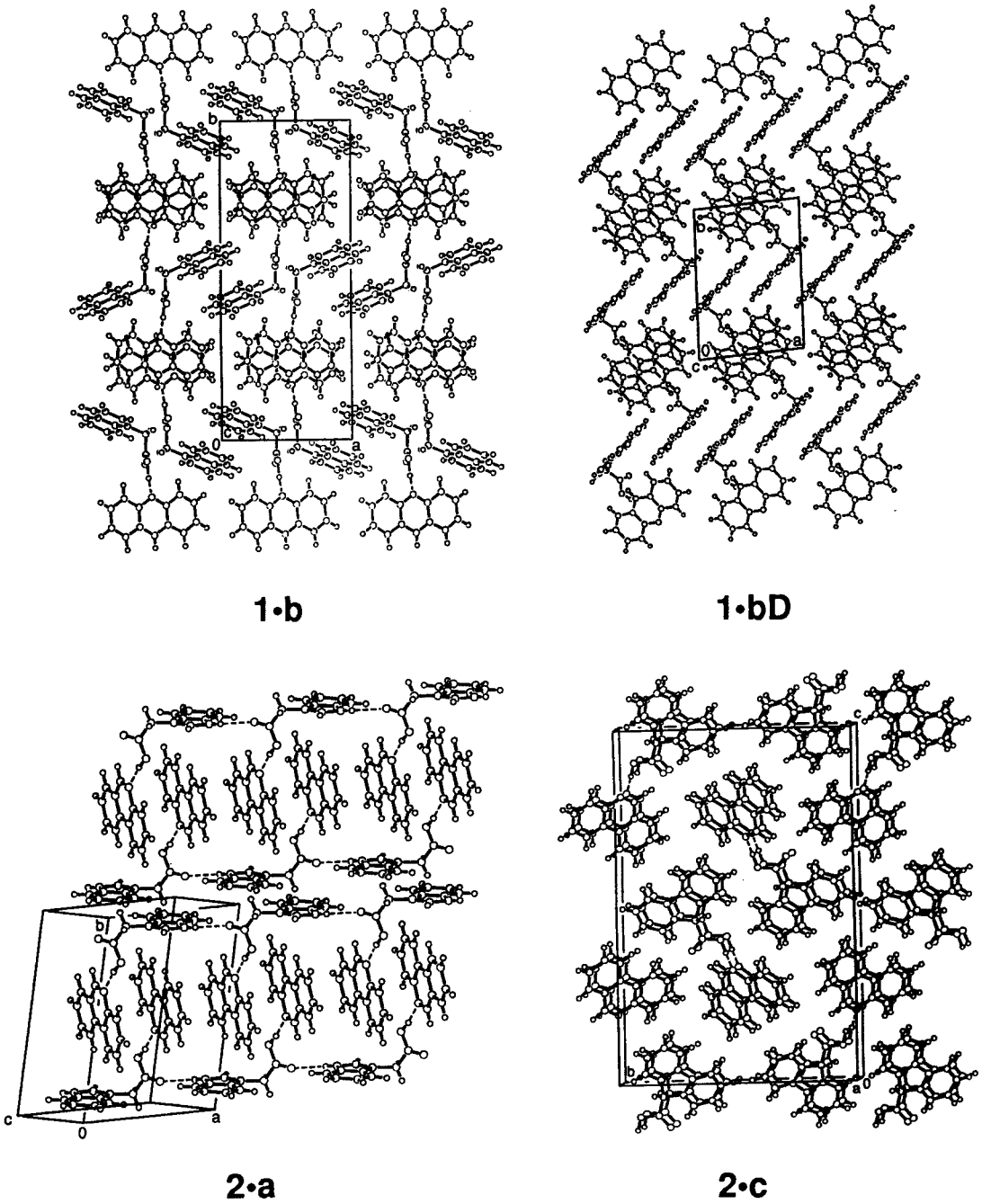

Figure 1. Molecular packing diagrams of the two-component molecular crystals **1·b**, **1·bD**, **2·a**, and **2·c**.

the crystal lattice (open arrow in Figure 2), assuming that the relative positions of these radical species formed in the crystal lattice have not changed much from those of the starting crystals.

On the other hand, radical coupling occurs between a geminate radical pair **15** and **13** or **14**, which are derived from a hydrogen bonding pair (C1- - -C2) or neighboring hydrogen bonding pairs (C1- - -C3), depending on the molecular arrangement in the crystal lattice. Only in the crystal **2·a** can the radical coupling occur between C1 and C2 within the geminate radical pair derived from a hydrogen bonding pair because the C1- - -C2 distance (5.34 Å) is shorter than the C1- - -C3 (8.04 Å) distance due to the head-to-tail stacking (Figure 2 and Table 6). In the crystals **1·a**, **1·b**, **1·bD**, and **1·d**, the C1- - -C3 coupling is preferred to the C1- - -C2 coupling because the head-to-tail stacking of hydrogen bonding pairs results in a shorter C1- - -C3 distance than the C1- - -C2 distance, and further the C1- - -C2 coupling should be accompanied by steric hindrance or half rotation of the acridine ring.

In the crystal lattice of **2·c**, the hydrogen bonding pairs of **2** and **c** are stacked in a head-to-head manner to make a column structure. The C1- - -C3 distance between the neighboring pairs in a single column is slightly shorter (4.75 Å) than the C1- - -C2 distance (5.23 Å) within a hydrogen bonding pair, resulting in the radical coupling between C1 and C3. The crystal **1·c** also has head-to-head stacking of the molecular pairs to form a column structure; the C1- - -C3 radical coupling between neighboring columns is caused because of the shorter C1- - -C3 distance (6.49 Å) than the C1- - -C2 distance (7.71 Å).

The fact that **2·e** showed no photoreactivity is difficult to explain from the molecular packing arrangement (Figure 2) because the C1- - -H1 (3.47 Å) and C1- - -C3 (4.53 Å) distances are short enough to cause hydrogen abstraction and radical coupling. The complete recovery of starting materials **2** and **e** means that any radical species such as **15** and **13** or **14** were not produced, probably due to the fast back-electron transfer of the radical anion **10** and the radical cation **11**.

Scheme 1

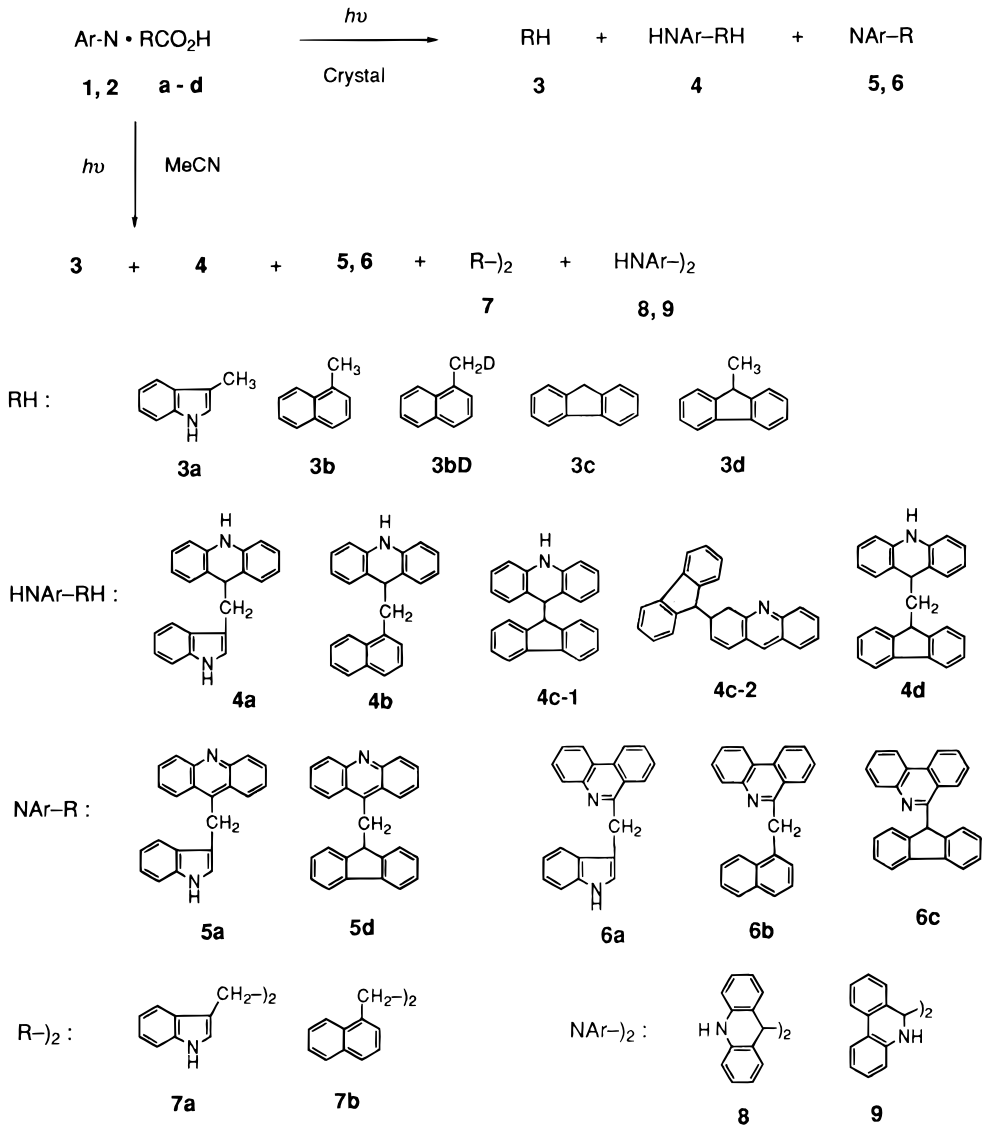

Table 4. Solution Photoreaction of Aza Aromatic Compounds and Aralkyl Carboxylic Acids at 15 °C

components (solvent)	conversion (%)		yield based on consumed acid (%)						
	1 or **2**	acid	**3**	**4**	**5**	**6**	**7**	**8**[a]	**9**[a]
1 + **a** (MeCN)	80	75	0	49	4		0	45	
1 + **a** (benzene)	64	33	0	18	40		0	52	
1 + **b** (MeCN)	81	87	2	70	0		10	12	
1 + **b** (benzene)	90	100	1	37	0		3	52	
1 + **c** (MeCN)	86	98	28	43,[b] 10[c]	0		0	6	
1 + **d** (MeCN)	75	67	21	30	26		0	37	
2 + **a** (MeCN)	15	25	14			35	35		23
2 + **b** (MeCN)	40	87	17			37	9		12
2 + **c** (MeCN)	11	99	85			10	0		0

[a] Yield based on consumed aza aromatic compound. [b] Compound **4c-1**. [c] Compound **4c-2**.

We could obtain the evidence that the radical **15** eventually abstracted the H1 hydrogen atom of the CO_2H group by irradiating the deuterated crystal **1·bD**. As shown in Table 5, **1·bD** similarly caused highly selective decarboxylation. The irradiated crystal was treated with CH_2N_2 immediately after the irradiation to prevent further photoreaction caused by diffused light, and the products were analyzed by GLC-MS and ^{1}H NMR spectrometry. The mass fragment data of a GLC peak corresponding to methylnaphthalene were *m*/*e* 143.15 (intensity 100.00), 142.14 (87.91), 116.10 (23.53), and 70.80 (33.83), giving an assignment as a 1-methylnaphthalene (CH_2D−) (**3bD**). For comparison, the mass fragment data obtained by the irradiation of **1·b** were 142.15 (100.00), 141.15 (86.56), 115.10 (30.19), and 70.40 (30.26). The ^{1}H NMR chemical shift of 1-C**H$_2$**D-Na was δ 2.67 (2H, m); and that of 1-C**H$_3$**-Na was 2.64 (3H, s). These results confirm that the hydrogen abstraction path in Figure 2 is correct.

Acridine (**1**) or phenanthridine (**2**) are regenerated by hydrogen abstraction from the radical species **13** or **14** in the solid state. Dimerization of **13** or **14** is not caused by their small mobility in the crystal lattice, despite the formation of dimers **8** or **9** in the solution photoreaction. In particular, after irradiation of **2·a** and **2·c** at −70 °C, **2** was completely recovered without any consumption. It means that the aza aromatic compounds behave like a sensitizer, acting only on one cycle, i.e. a stoichiometrical sensitizer. Such stoichiometrical sensitization is a new concept, which is specific in the solid state photochemistry.

Conclusions

A series of two-component molecular crystals of aza aromatic compounds and aralkyl carboxylic acids were prepared by recrystallization from the solutions. Irradiation of the crystals at lower temperatures caused more selective and efficient decarboxylation to give finally the decarboxylated products

Table 5. Photoreaction of the Two-Component Molecular Crystals of Aza Aromatic Compounds and Aralkyl Carboxylic Acids

crystal	irrad temp (°C)	conversion (%)		yield based on consumed acid (%)			
		1 or **2**	acid	**3**	**4**	**5**	**6**
1·a	−70	12	10	90	5	0	
1·a	−50	12	12	83	7	7	
1·a	−30	9	15	73	12	4	
1·a	−10	6	25	73	12	4	
1·a	15	29	86	71	12	1	
1·b	−70	19	50	81	4	0	
1·b	15	36	85	61	15	0	
1·bD	−70	9	30	88[a]	3	0	
1·bD	−10	14	63	68[a]	5	0	
1·c	−70	4	5	94	0	0	
1·c	−30	4	13	94	0	0	
1·c	15	29	92	82	10[b]	0	
1·d	−70	4	12	93	0	0	
1·d	−30	8	46	73	0	0	
1·d	15	20	61	77	5	7	
2·a	−70	0	23	92			0
2·a	−50	3	38	89			5
2·a	−30	4	40	92			7
2·a	−10	5	51	81			7
2·a	15	14	62	69			13
2·a	15	20	91	77			10
2·b	−70	5	35	93			4
2·b	15	30	80	68			16
2·c	−70	0	30	98			0
2·c	−30	3	35	95			3
2·c	15	2	100	97			2

[a] 1-Methyl(CH_2D)naphthalene **3bD**. [b] Compound **4c-1**.

Scheme 2

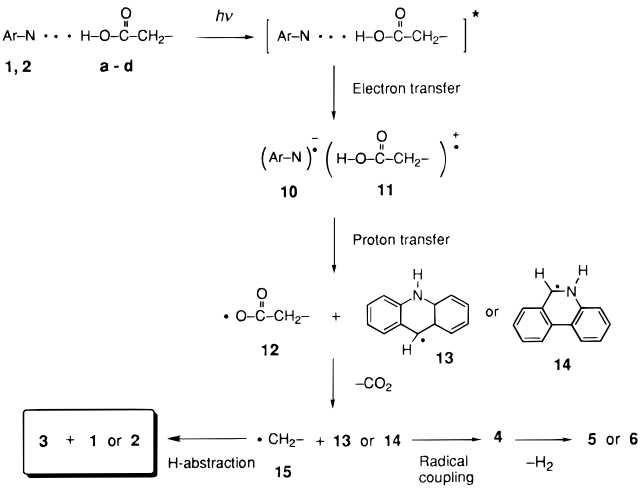

Table 6. Estimated Distances for Hydrogen Abstraction and Radical Coupling

distance[a] (Å)	**1·a**	**1·b**	**1·bD**	**1·c**	**1·d**	**2·a**	**2·c**	**2·e**
Hydrogen Abstraction within H-Bonding Pair								
C1- - -H1	3.33	3.47	3.20[b]	3.31	3.30	3.18	3.40	3.47
Radical Coupling within H-Bonding Pair								
C1- - -C2	7.40	7.57	7.75	7.71	7.53	5.34	5.23	5.39
Radical Coupling between Neighboring H-Bonding Pairs								
C1- - -C3	5.95	6.06	5.08	6.49	5.41	8.04	4.75	4.53

[a] See Figure 2 for the numbering. [b] H is exchanged to D.

alone in high yields. Aza aromatic compounds play the role of stoichiometrical sensitizer, which can act only in one cycle in the crystal lattice.

Experimental Section

General Procedures. ^{1}H-NMR spectra were measured on a 60-MHz JEOL spectrometer with tetramethylsilane as an internal standard. IR spectra were recorded on a JASCO FT/IR-8300 spectrophotometer. UV spectra were measured on a Shimadzu UV-3100 spectrophotometer. Mass spectra were taken on a Shimadzu PARVUM QP-5000 GLC-MS. Differential scanning calorimetry (DSC) was done on a Rigaku Thermoflex TAS-200 DSC8230D and melting points (mp) were not corrected. Elemental analysis was carried out with a Yanaco CHN Corder MT-5. HPLC with a photodiode-array detector were used for determining the products on a Waters HPLC system. All the reagents were commercially available.

Preparation of Two-Component Molecular Crystals of Aza Aromatic Compounds (1, 2) and Aralkyl Carboxylic Acids (a−e). Nine two-component molecular crystals of aza aromatic compounds and aralkyl carboxylic acids were prepared by slow evaporation at room temperature or with gentle heating of the equimolar solutions (Chart 1). Deuterated 1-naphthylacetic acid (**bD**, mp 125−128 °C) was prepared by exchanging the CO_2H carboxylic acid group with CO_2D in MeOD followed by dryness. A crystal of **1·bD** was obtained by recrystallization from a 1:1 solution of **1** and **bD** in benzene−cyclohexane (1:1) shaken once with D_2O. The solvents for crystallization, melting points, and elemental analyses of the crystals are summarized in Table 1.

Preparative Photoreaction in Solutions. For the common procedure, a solution (100 mL) of an aza aromatic compound (5 mmol) and a carboxylic acid (5 mmol) was internally irradiated with a 100-W high-pressure mercury lamp under argon at room temperature. The reaction mixture was filtered to separate a precipitate of **8** or **9** and the solution was submitted to preparative TLC (silica gel plate, benzene−ethyl acetate), and in some cases preparative HPLC (C_{18} column, MeOH−H_2O) was subsequently carried out.

Irradiation of **1** (895 mg) and **a** (875 mg) in MeCN for 2 h gave **4a**·$^1/_2CCl_4$ (1270 mg), **5a**·cyclohexane (174 mg), and **8** (95 mg) in 66%, 9%, and 11% yields, respectively. **4a**·$^1/_2CCl_4$: mp 171−172 °C (from 1:3 CH_2Cl_2−CCl_4); ^{1}H NMR (acetone-d_6) δ 9.73 (broad, 1H), 7.80 (broad, 1H), 6.50−7.50 (m, 13H), 4.30 (t, J = 7.0 Hz, 1H), 2.95 (d, J = 7.0 Hz, 2H); IR (KBr) 3419, 3371, 1609, 1454, 1301, 1095, 789 cm^{-1}; UV (MeCN) λ_{max} 208 (log ϵ 4.85), 222 (4.63), 282 nm (4.34). Anal. Calcd for $C_{22}H_{18}N_2$·$^1/_2CCl_4$: C, 69.78; H, 4.68; N, 7.23. Found: C, 70.06; H, 5.30; N, 7.45. C, H, and N all had higher found than calculated values. Possibly it is easy to lose CCl_4. **5a**·cyclohexane: mp 228−230 (from 1:3 THF−cyclohexane); ^{1}H NMR (THF-d_8−MeCN-d_3) δ 7.00−8.50 (m, 12H), 6.30 (m, 1H), 5.10 (d, J = 1.5 Hz, 2H), 1.45 (s, 12H); IR (KBr) 3080, 2845, 1611, 1518, 1457, 1354, 1227, 824 cm^{-1}; UV (MeCN) λ_{max} 221 (log ϵ 4.70), 252 (5.15), 360 (3.96), 383 nm (3.73). Anal. Calcd for $C_{22}H_{16}N_2$·C_6H_{12}: C, 85.67; H, 7.19; N, 7.14. Found: C, 85.47; H, 7.18; N, 7.27. The molecular structure of **5a** was confirmed by X-ray structure analysis of **5a**·cyclohexane (Scheme 1, Table 2). **8**: mp 211−212 °C (from THF). The IR spectrum and elemental analysis of **8** were consistent with those of the authentic sample.[5c]

Irradiation of **1** (895 mg) and **b** (930 mg) in benzene for 1 h gave **3b** (7 mg), **4b** (750 mg), **7b** (18 mg), and **8** (327 mg) in 1%, 37%, 3%, and 47%, respectively. **4b:** mp 180−181 °C (from benzene); ^{1}H NMR (acetone-d_6) δ 6.53−8.15 (m, 15H), 4.33 (t, J = 7.0 Hz, 1H), 3.20 (d, J = 7.0 Hz, 2H); IR (KBr) 3373, 3040, 2925, 2900, 2860, 1606, 1578, 1472, 790 cm^{-1}; UV (MeCN) λ_{max} 210 (log ϵ 4.83), 223 (4.83), 223 (4.88), 279 nm (4.35). Anal. Calcd for $C_{24}H_{19}N$: C, 89.68; H, 5.96; N, 4.36. Found: C, 89.91; H, 6.28; N, 4.32. **7b:** ^{1}H NMR ($CDCl_3$) δ 6.80−8.20 (m, 14H), 3.50 (s, 4H); IR (KBr) 3035, 1586, 1460, 1394, 786 cm^{-1}. The structure of **7b** was tentatively given.

Irradiation of **1** (895 mg) and **c** (930 mg) in MeCN for 2 h gave **3c** (265 mg), **4c-1** (683 mg), **4c-2** (140 mg), and **8** (100 mg) in 32%, 40%, 8%, and 11% yields, respectively. **3c:** mp 111−112 °C. The ^{1}H NMR and IR spectral data are consistent with those of an authentic sample. **4c-1:** mp 245−246 °C (from 1:1 THF−MeCN); ^{1}H NMR (DMSO-d_6) δ 8.55 (s, 1H), 6.10−8.00 (m, 16H), 5.00 (d, J = 3.8 Hz, 1H), 4.17 (d, J = 3.8 Hz, 1H); IR (KBr) 3390, 3035, 1608, 1488, 1310, 742 cm^{-1}; UV (MeCN) λ_{max} 208 (log ϵ 4.84), 250 (4.19), 277 nm (4.38). Anal. Calcd for $C_{26}H_{19}N$: C, 90.40; H, 5.54; N, 4.05. Found: C, 90.49; H, 5.65; N, 3.98. **4c-2:** mp 167−170 °C (from 1:3 THF−MeCN); ^{1}H NMR ($CDCl_3$) δ 7.00−8.00 (m, 13H), 6.65 (dd, J = 10.0, 2.0 Hz, 1H), 6.20 (dd, J = 9.5, 2.0 Hz, 1H), 4.30 (d, J = 3.8 Hz, 1H), 3.73 (m, 1H), 2.80 (s, 1H), 2.67 (d, J = 3.8 Hz, 1H); IR (KBr) 3030,

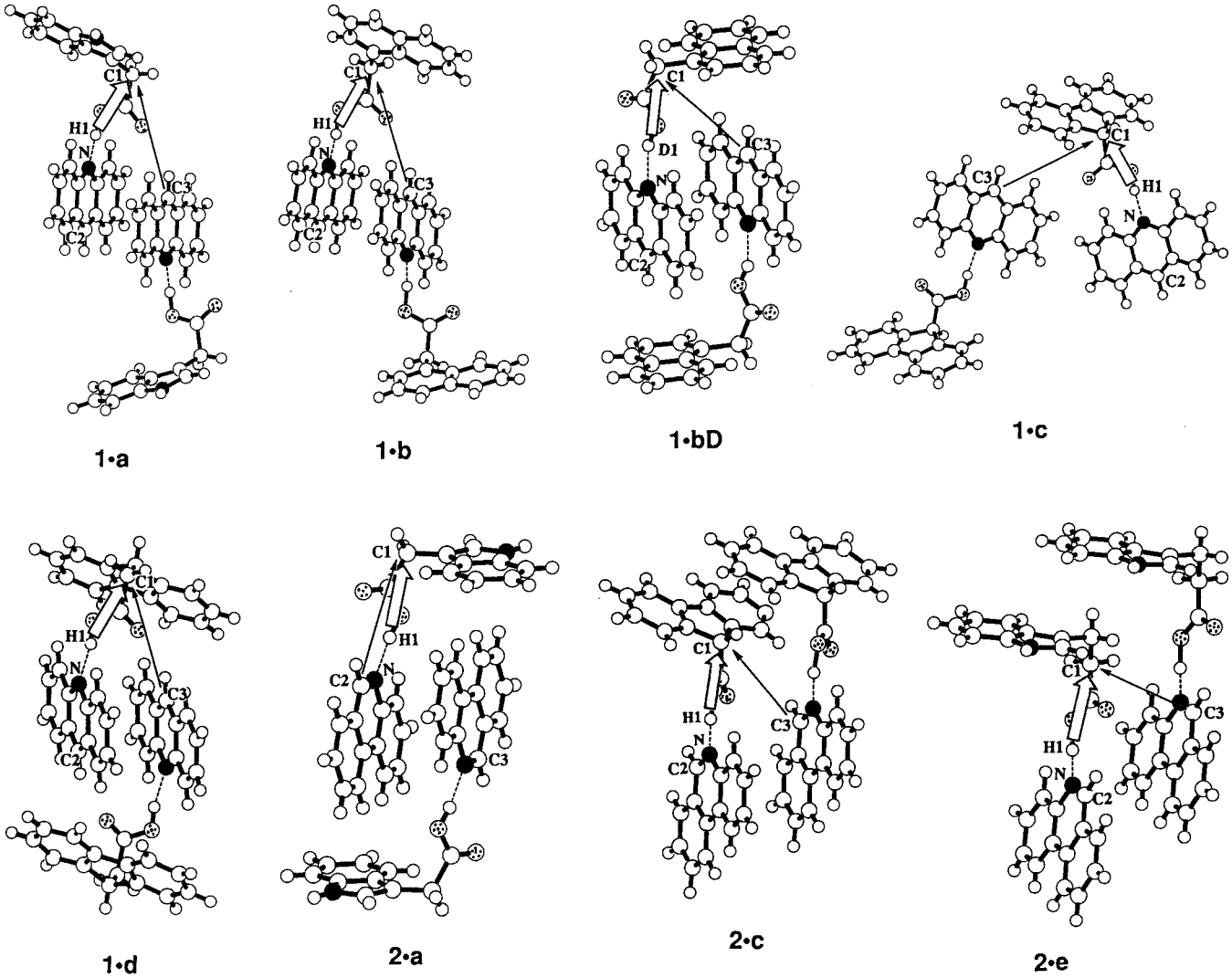

Figure 2. Reaction path in the crystal lattice. The atom numbers correspond to those in Table 6. Black and dotted atoms identify N and O atoms, respectively.

2860, 1610, 1486, 910, 760 cm^{-1}; UV (MeCN) λ_{max} 210 (log ϵ 4.73), 223 (4.64), 255 (4.70), 291 (4.33), 329 (3.76), 344 (3.76). Anal. Calcd for $C_{26}H_{19}N$: C, 90.40; H, 5.54, N, 4.05. Found: 90.68; H, 5.67; N, 4.12. The molecular structure of **4c-2** was determined by X-ray crystallographic analysis for the verification (Scheme 1, Table 2).

Photoreaction of **1** (895 mg) and **d** (1121 mg) in MeCN for 14 h gave **3d** (15 mg), **4d** (144 mg), **5d** (170 mg), and **8** (115 mg) in 3%, 8%, 10%, and 13% yields, respectively. **3d:** mp 44−45 °C; ^{1}H NMR ($CDCl_3$) δ 7.18−7.85 (m, 8H), 3.90 (t, J = 7.5 Hz, 1H), 1.50 (d, J = 7.5 Hz, 3H). **4d:** white powder, mp 248−250 °C (from MeOH); ^{1}H NMR ($CDCl_3$) δ 6.60−8.33 (m, 16H), 6.10 (s, broad, 1H), 3.74−4.15 (m, 2H), 2.10 (q, J = 6 Hz, 2H); IR (KBr) 3400, 3055, 1606, 1500, 1440, 1308, 740 cm^{-1}; UV (MeCN) λ_{max} 208 (log ϵ 4.91), 268 nm (4.46). Anal. Calcd for $C_{27}H_{21}N$: C, 90.21; H, 5.89; N, 3.90. Found: C, 90.39; H, 5.95; N, 3.65. **5d:** pale yellow crystal, mp 215−217 °C (from MeCN); ^{1}H NMR (THF-d_8) δ 6.60−8.43 (m, 16H), 4.50 (t, J = 7.8, 1H), 4.00 (d, J = 7.8 Hz, 2H); IR (KBr) 3060, 1608, 1550, 1513, 1472, 1404 750 cm^{-1}; UV (MeCN) λ_{max} 209 (log ϵ 4.77), 253 (5.16), 359 (3.99). Anal. Calcd for $C_{27}H_{21}N$: C, 90.72; H, 5.36; N, 3.92. Found: C, 90.36; H, 5.40; N, 3.65.

Photoreaction of **2** (895 mg) and **a** (875 mg) in MeCN for 10 h gave **3a** (84 mg), **6a** (305 mg), **7a** (96 mg), and **9** (370 mg) in 13%, 20%, 15%, and 41% yields, respectively. **6a:** mp 202−204 °C (from MeCN); ^{1}H NMR ($CDCl_3$) δ 6.90−8.67 (m, 13H), 6.60−6.73 (m, 1H), 4.80 (d, J = 2 Hz, 2H); IR (KBr) 3230, 3065, 1608, 1520, 1452, 1366, 1224, 1104, 762 cm^{-1}; UV (MeCN) λ_{max} 221 (log ϵ 4.76), 248 (4.69), 329 (3.43), 343 nm (3.36). Anal. Calcd for $C_{22}H_{16}N_2$: C, 85.69; H, 5.23; N, 9.08. Found: C, 85.78; H, 5.46; N, 9.08. **7a:** mp 263−265 °C (from MeCN); ^{1}H NMR (THF-d_8) δ 9.73 (s, broad, 2H), 6.83−7.67 (m, 10H), 3.10 (s, 4H); IR (KBr) 3400, 3050, 1614, 1454, 1334, 1220, 1090, 744 cm^{-1}; UV (MeCN) λ_{max} 225 (log ϵ 4.86), 282 (4.11). Anal. Calcd for $C_{18}H_{16}N_2$: C, 83.04; H, 6.19; N, 10.76. Found: C, 82.63; H, 6.33; N, 10.90. **9:** mp 230 °C dec; IR (KBr) 3380, 3340, 3070, 1603, 1465, 1280, 755 cm^{-1}. Anal. Calcd for $C_{26}H_{20}N_2$: C, 86.63; H, 5.59; N, 7.77. Found: 86.16; H, 5.83; N, 8.04. The structure of **9** was tentatively given.

Irradiation of **2** (895 mg) and **b** (930 mg) in MeCN for 10 h gave **3b** (54 mg), **6b** (692 mg), **7b** (13 mg), and **9** (250 mg) in 8%, 43%, 2%, and 28% yields, respectively. **6b:** 143−145 °C (from 1:1 CH_2Cl_2−hexane); ^{1}H NMR ($CDCl_3$) δ 6.84−8.70 (m, 15H), 5.16 (s, 2H); IR (KBr) 3045, 1608, 1480, 1164, 792 cm^{-1}; UV (MeCN) λ_{max} 224 (log ϵ 4.97), 249 (4.65), 272 (4.24), 344 nm (3.23). Anal. Calcd for $C_{24}H_{17}N$: C, 90.28; H, 5.33; N, 4.39. Found: C, 90.04; H, 5.67; N, 4.30.

Irradiation of **2** (895 mg) and **c** (1050 mg) in MeCN for 9 h gave **3c** (750 mg), **6c** (134 mg), and **9** (60 mg) in 90%, 8%, and 7% yields, respectively. **3c:** mp 113−116 °C. The ^{1}H NMR and IR spectra of **3c** are identical with those of an authentic sample. **6c:** mp 225−228 °C (from 1:3 THF−MeCN); ^{1}H NMR (THF-d_8) δ 6.50−8.80 (m, 16H), 5.90 (s, broad, 1H); IR (KBr) 3075, 1608, 1570, 1478, 1350, 754 cm^{-1}; UV (MeCN) λ_{max} 208 (log ϵ 4.81), 252 (4.80), 301 (4.09). Anal. Calcd for $C_{26}H_{17}N$: C, 90.90; H, 4.99; N, 4.08. Found: C, 90.80; H, 5.09; N, 4.12.

HPLC Study of Photoreaction in MeCN. A MeCN solution (10 mL) of 0.05 M aza aromatic compound and 0.05 M aralkyl carboxylic acid in a Pyrex test tube was externally irradiated with a 400-W high-pressure mercury lamp under argon bubbling for 1−15 h at 15 °C. After the reaction mixture was filtered off to remove **8** or **9**, the solution

was methylated with CH_2N_2 and analyzed by HPLC. The results are shown in Table 4.

Solid State Photoreaction of the Two-Component Molecular Crystals. A crystal (20 mg) was pulverized in a mortar, placed between two Pyrex glass plates in a circle 5 cm in diameter, and irradiated with a 500-W xenon short arc lamp with a UV transparent filter (290−400 nm irradiation) or a 400-W high-pressure mercury lamp (>290 nm irradiation) under argon at various temperatures in the range −70 to 15 °C for 1−3 h. The irradiated mixture was treated with CH_2N_2 and then analyzed by HPLC. The results are listed in Table 5. For the crystals **1·b** and **1·bD**, the mass spectra were also measured by GC-MS immediately after the irradiation followed by methylation with CH_2N_2.

X-ray Crystallographic Analyses. Data collections were performed with a Riguku AFC7R automatic four-circle X-ray diffractometer and a rotating anode equipped with a graphite monochromated Mo Kα (λ = 0.71069 Å) or Cu Kα (λ = 1.54178 Å) radiation. Three standard reflections were monitored every 150 measurements for all data collections, and no degradation was ascertained. Absorption correction was applied. These structures were solved by direct methods and expanded by using Fourier techniques. The non-hydrogen atoms were refined anisotropically. Atomic parameters were refined by the full-matrix least-squares method at the final stage. All the calculations were carried out with use of the teXsan crystallographic software package, Molecular Structure Corporation.

The crystals **1·bD** and **5a·**cyclohexane were measured in glass capillaries to prevent the degradation. Detailed crystal data for the ten two-component molecular crystals and the photoproducts **5a·**cyclohexane and **4c-2** are summarized in Table 2.

Acknowledgment. This work was supported by PRESTO, Japan Science and Technology Corporation, and a Grant-in-Aid for scientific research from the Ministry of Education, Science and Culture, Japan. One of the authors (K.D.) is a guest researcher from Zhengzhou University, China.

Supporting Information Available: Tables giving full data collection parameters and further details of refinement, atomic coordinates, anisotropic displacement parameters, bond lengths and angles, and torsion angles of **1·a**, **1·b**, **1·bD**, **1·c**, **1·d**, **2·c**, **4c-2**, and **5a·**C_6H_{12} (132 pages). See any current masthead page for ordering and Internet access instructions.

JA971156A